

Article

Lost, but found with Nile red; a novel method to detect and quantify small microplastics (20 μm –1 mm) in environmental samples

Gabriel Erni-Cassola, Matthew I. Gibson, Richard C. Thompson, and Joseph christie-oleza

Environ. Sci. Technol., **Just Accepted Manuscript** • DOI: 10.1021/acs.est.7b04512 • Publication Date (Web): 07 Nov 2017

Downloaded from <http://pubs.acs.org> on November 8, 2017

Just Accepted

“Just Accepted” manuscripts have been peer-reviewed and accepted for publication. They are posted online prior to technical editing, formatting for publication and author proofing. The American Chemical Society provides “Just Accepted” as a free service to the research community to expedite the dissemination of scientific material as soon as possible after acceptance. “Just Accepted” manuscripts appear in full in PDF format accompanied by an HTML abstract. “Just Accepted” manuscripts have been fully peer reviewed, but should not be considered the official version of record. They are accessible to all readers and citable by the Digital Object Identifier (DOI®). “Just Accepted” is an optional service offered to authors. Therefore, the “Just Accepted” Web site may not include all articles that will be published in the journal. After a manuscript is technically edited and formatted, it will be removed from the “Just Accepted” Web site and published as an ASAP article. Note that technical editing may introduce minor changes to the manuscript text and/or graphics which could affect content, and all legal disclaimers and ethical guidelines that apply to the journal pertain. ACS cannot be held responsible for errors or consequences arising from the use of information contained in these “Just Accepted” manuscripts.



1 **Lost, but found with Nile red; a novel method to detect and quantify**
2 **small microplastics (20 μm –1 mm) in environmental samples**

3 Gabriel Erni-Cassola^{1*}, Matthew I. Gibson^{2,3}, Richard C. Thompson⁴, Joseph A. Christie-
4 Oleza^{1*}

5

6 ¹ School of Life Sciences, University of Warwick, Coventry CV4 7AL, UK.

7 ² Department of Chemistry, University of Warwick, Coventry CV4 7AL, UK.

8 ³ Warwick Medical School, University of Warwick, Coventry CV4 7AL, UK.

9 ⁴ School of Biological and Marine Sciences, Plymouth University, Plymouth PL4 8AA, UK.

10

11 *corresponding authors at: School of Life Sciences, University of Warwick, Coventry CV4
12 7AL, UK.

13 gabriel.ernicassola@gmail.com / g.ernicassola@warwick.ac.uk and J.Christie-
14 Oleza@warwick.ac.uk

15

16 **Abstract**

17 Marine plastic debris is a global environmental problem. Surveys have shown that plastic
18 particles <5 mm in size, known as microplastics, are significantly more abundant in surface
19 seawater and on shorelines than larger plastic particles. Nevertheless, quantification of
20 microplastics in the environment is hampered by a lack of adequate high throughput methods
21 to distinguish and quantify smaller size fractions (<1 mm), and this has probably resulted in
22 an underestimation of actual microplastic concentrations. Here we present a protocol that
23 allows high throughput detection and automated quantification of small microplastic particles
24 (20–1000 μm) using the dye Nile red, fluorescence microscopy and image analysis software.
25 This protocol has proven highly effective in the quantification of small polyethylene,
26 polypropylene, polystyrene and nylon 6 particles, which frequently occur in the water
27 column. Our preliminary results from sea surface tows show a power-law increase of small
28 microplastics (*i.e.* <1 mm) with decreasing particle size. Hence, our data helps to resolve
29 speculation on the ‘*apparent*’ loss of this fraction from surface waters. We consider that this
30 method presents a step change in the ability to detect small microplastics by substituting the
31 subjectivity of human visual sorting with a sensitive and semi-automated procedure.

32

33 Introduction

34 It has been estimated that mismanagement of plastic waste resulted in up to 12.7
35 million tonnes of plastic entering the ocean in 2010 alone.¹ In the environment, plastics
36 accumulate due to their recalcitrant nature, contaminating sediments and surface seawaters on
37 a global scale.^{2,3} In aquatic systems, polymer types with lower density than seawater have a
38 higher transportability (*via* rivers⁴ into marine coastal areas and oceanic gyres)⁵ than higher
39 density polymers, which tend to settle out.⁶⁻⁸ Lower density plastics, such as polypropylene
40 (PP), polyethylene (PE) and certain forms of polystyrene (PS) are frequently used as
41 packaging materials⁹ and hence, have a very short service life prior to disposal. These types of
42 plastic are also more commonly found in environmental surveys.^{10,11}

43 Eriksen *et al.*¹² estimated that about 5.25 trillion plastic fragments are currently
44 floating on the ocean's surface. Extensive sampling of surface seawater and comparison
45 across all size classes (>200 μm) has shown that plastic particles <5 mm are significantly
46 more abundant than larger particles.^{5,12,13} These plastic fragments (<5 mm) have been termed
47 microplastics.^{14,15} Marine microplastics are composed of two main types: (1) primary
48 microplastics that stem directly from the source, such as microbeads contained in cosmetics,
49 or fibres released during washing of synthetic garments,¹⁶ and (2) secondary microplastics
50 that are generated through macroplastic fragmentation, a break down process influenced by
51 UV-irradiation, high temperatures and mechanical shear forces.^{17,18} Morét-Ferguson *et al.*¹⁹,
52 found that the average size of buoyant plastic particles in the Northern Atlantic and Caribbean
53 had halved in size from an average 10 mm in the 1990s to 5 mm in the 2000s. The decrease in
54 average size of plastic marine debris is of concern because the smaller synthetic polymers are
55 ingested by relatively more organisms at the base of the marine food web.³ Recent studies
56 suggest that ingested particles can be transferred between trophic levels^{20,21} and transport
57 persistent organic pollutants.²² The possible environmental effects of microplastics has led to
58 growing public and media attention as well as policy measures to reduce inputs, such as
59 banning the use of plastic microbeads in personal care products.²³ Besides these concerns and
60 abatement measures, monitoring of marine litter is currently required in the EU under the

61 Marine Strategy Framework Directive (MSFD)²⁴ and it is therefore essential to have reliable,
62 reproducible, rapid and inexpensive methods for quantification and monitoring of
63 microplastic contamination in the environment.

64 Current methodology for quantification of environmental microplastic contamination
65 is hampered by a lack of methods that are both sensitive and allow high throughput
66 quantification. Commonly applied methods separate synthetic microparticles from non-
67 synthetic materials *via* density separation and floatation techniques, before visually sorting
68 the particles and finally confirming their identity with spectroscopy.²⁵ The data generated can
69 result in an underestimate of small microplastics because of the visual step in the process.²⁶
70 Alternative, faster and less expensive protocols are of particular importance for routine
71 monitoring of plastic contamination by regulatory bodies and the need for developing new
72 methods has been clearly identified as a policy priority (MSFD).²⁴ Here, we adopt the
73 sampling criteria proposed by the EU technical subgroup on marine litter,²⁴ who recommend
74 two categories: *large* microplastics ranging from 5 mm–1 mm in size (visually recognizable)
75 and *small* microplastics ranging from 1 mm–20 μm for which reliable quantification is still
76 challenging.

77 In this study, we present the application of a fluorescence-based protocol using Nile
78 red to detect and quantify small microplastics in environmental samples. This method is
79 inexpensive, employs readily available equipment and can be semi-automated for high
80 throughput sample analysis. The method requires a sample purification step, fluorescence
81 microscopy (green fluorescence protein settings) and free image analysis software.

82 **Materials and Methods**

83

84 *Microplastic staining and quantification protocol validation using commercial synthetic*
85 *polymers*

86

87 Nile red had been suggested as a tool to fluorescently label microplastics^{18,27}, and its use was
88 later demonstrated.^{28,29} The dye is commonly dissolved in acetone,³⁰ but here methanol was
89 chosen because common plastics are resistant to it. The fluorescence of Nile red is influenced
90 by its concentration, which lies optimally between 0.1 and 2 $\mu\text{g mL}^{-1}$,³⁰ and higher
91 concentrations lead to quenching.³⁰ Accordingly, the working solution for this study was
92 prepared by dissolving Nile red (technical grade, N3013, Sigma-Aldrich) in methanol to a
93 concentration of $1\mu\text{g mL}^{-1}$.

94 Staining efficacy and automated particle detection was tested on nine different
95 polymer types: PE (powder, ~40–48 μm , Sigma-Aldrich), poly(ethylene terephthalate) (PET,
96 powder, $\leq 300\ \mu\text{m}$, GoodFellow), PVC (powder, ~80–148 μm , Sigma-Aldrich), nylon 6
97 (pellets, ~1 mm, Sigma-Aldrich), PP (pellets, ~7 mm, Sigma-Aldrich), PS (pellets, ~5 mm,
98 Sigma-Aldrich), PC (fragment from panel, ~10 mm), polyurethane (PUR, pellets, ~3 mm,
99 Sigma-Aldrich), and black tire rubber (fragment from bicycle tire, 7×4 mm). Nylon 6
100 microplastics were prepared by heating the pellets and pulling them apart to produce thin
101 fibres, which then were cut to microparticles (~63–91 μm) under a dissection microscope. PP
102 pellets as well as black rubber were ground in liquid nitrogen with mortar and pestle to obtain
103 small microplastic fragments (PP: ~20–130 μm , black rubber: ~57–171 μm). PS and PC
104 microparticles were obtained by sanding the pellets with a metal file and further cutting the
105 obtained particles with a scalpel under a dissection microscope to the final sizes (PS: ~24–196
106 μm , PC: ~94–169 μm). PUR pellets were directly cut to size under a dissection microscope
107 (~71–154 μm). Sizes of all microparticles produced in the laboratory were calculated from the
108 square root of particle area, which was measured in ImageJ using brightfield microscope
109 images. Ten particles of each polymer type were placed on separate clean PC track-etched

110 filter membranes (PCTE, 25 mm diameter, 10 μm pore size, Whatman) to evaluate the
111 efficiency of detection of our protocol. PCTE filters are optimal for two reasons: (1) their
112 hydrophilic surface avoids Nile red background fluorescence and (2) translucent properties
113 when exposed to methanol allow brightfield microscopy in addition to fluorescence
114 microscopy. About 2–3 drops of Nile red solution were carefully added to cover each filter.
115 Filters were placed on standard microscope slides, covered with cover slips and fixed with
116 tape to avoid movement of the sample. The samples were then maintained for 10 minutes at
117 60 °C in the dark.

118 Microscopic imaging was performed using a light microscope (Nikon Eclipse Ti)
119 equipped with a widefield camera (Andor Zyla sCMOS) and a LED for fluorescence. We
120 tested the fluorescence of the nine different polymers stained with Nile red on PCTE filters in
121 green (excitation/emission 460/525 nm) and red (565/630 nm). Green fluorescence was
122 chosen over red fluorescence because (1) synthetic polymers either fluoresced better in green
123 (fig. S1 a-d) or fluorescence did not differ significantly (fig. S1 e), (2) natural contaminants
124 fluoresced in red but not in green after hydrogen peroxide (H_2O_2) digestion (fig. S2, discussed
125 below) and (3) background signal from the filter membrane was lower. Three types of whole
126 filter images were obtained for each polymer type: red and green fluorescence, as well as
127 brightfield, all at a magnification of 10 \times . Exposure time for fluorescence was 30 ms at 30%
128 LED strength.

129 Automated particle recognition and quantification based on the fluorescent images
130 was performed in ImageJ (v1.50i). A macro was written to perform the following tasks: (1)
131 set the scale, (2) subtract the background using a rolling ball radius of 1500 pixels, (3)
132 convert images to 8bit, (4) adjust black and white thresholds using 29 and 175 as the lower
133 and higher values of pixel brightness, and finally (5) quantify particles based on area ($400 - \infty$
134 μm^2). The size detection limit was set to 400 μm^2 to ensure that pores from the filter
135 membrane (diameter = 10 μm) did not interfere in particle measurements.

136

137 *Validation of the pre-staining digestion protocol*

138

139 To prevent overestimation of synthetic particles in environmental samples, it is of critical
140 importance that biogenic materials, such as lipids, chitin or wood lignin, which fluoresce
141 when stained with Nile red (fig. S2 a, c), are eliminated or cease to fluoresce when stained.
142 While digestion with nitric acid proved highly efficient at removing biogenic matter, its
143 application is limited due to pH-sensitive polymers, such as PS particles, which melt together,
144 or Nylon fibres, which are lost during the process.³¹ A chemical alternative is given with
145 H₂O₂ treatments, against which common synthetic polymers are resistant.^{31,32} Hence,
146 digestion of biogenic material was performed as previously described by Claessens *et al.* with
147 slight modifications.³¹ Briefly, 20 ml of 30% H₂O₂ was added to 250 mL Erlenmeyer flasks
148 containing the filtered samples on PCTE filters, which were then kept at 60 °C for 1 h
149 followed by a prolonged 7 h step at 100 °C. Following the digestion, PCTE filters were
150 thoroughly rinsed with Milli-Q water and then removed. The remaining solution was filtered
151 through a new PCTE filter rinsing all particles from the flask and filtering device with Milli-
152 Q water. The new PCTE filter containing all collected material was stored in Petri dishes until
153 Nile red analysis.

154 The effect of the H₂O₂ digestion protocol on natural polymers was tested with the two
155 most commonly occurring natural polymers: chitin (powder, Sigma-Aldrich) and wood lignin
156 (below 1 mm in size; kindly provided by Prof. Tim Bugg and prepared according to
157 literature).³³

158

159 *Validation of the fluorescent-staining protocol with environmental samples*

160

161 Net tow and beach sand samples were obtained in June 2016 to test our fluorescent-labelling
162 method with environmental samples. Tow samples were collected from within Plymouth
163 Sound, UK. Five consecutive trawls of 15 min were undertaken with a manta net (0.50 m by
164 0.15 m mouth, 300 µm mesh) at a ship speed of 4 knots. After each tow, the collected
165 material was transferred into a container by rinsing the net and cod end with seawater. In the

166 laboratory, all material was pre-filtered through a 1 mm metallic mesh to eliminate large
167 debris. Retained debris was thoroughly washed with Milli-Q water to extract all small
168 microplastics. Retained debris was visually examined for plastic debris (fig. S3). The flow
169 through containing plastic particles <1 mm was vacuum filtered through PCTE filters (47 mm
170 diameter, 10 μm pore size, Whatman). All filters were placed into a 250 mL flask.

171 Sediment samples were collected from a beach at Bigbury (UK, 50°16'53N,
172 3°53'42W) by transferring the top 1 cm layer of five 30 x 30 cm² plots with a metallic spoon
173 into 500 mL glass bottles. Microplastics were extracted from sand samples according to the
174 density-separation/floatation protocol described in Nuelle *et al.*³⁴ using NaCl (26% w/v)
175 instead of NaI. The collected supernatant was vacuum filtered through PCTE filters, which
176 were placed in a 250 mL flask. Flasks containing the PCTE filters from net tows and beach
177 sand samples were stored at 60 °C during 24 h for desiccation. The H₂O₂ digestion, staining
178 and imaging was performed as described above.

179 Micro-Raman spectroscopy was used to verify the identity of the fluorescing and
180 non-fluorescing particles found on the filters in order to ascertain the specificity of Nile red to
181 only stain particles of synthetic origin. In total, 23 fields (23 × 1.8 mm²) from 6 different filter
182 sections (4 sediment samples, 2 water samples) were imaged as described above. Raman
183 spectra were acquired using an inVia Raman microscope (Renishaw). Raman shifted spectra
184 were recorded using a 442 nm excitation laser in a range of 100 to 3500 waves cm⁻¹ and 10 s
185 exposure time accumulating 20 scans. Particles were bleached during 5 min prior to spectrum
186 acquisition as Nile red fluorescence interfered with the Raman signal. The baselines of
187 Raman spectra were corrected in R (v3.2.3)³⁵ using the peak detection method from the
188 baseline package³⁶ and then normalized.

189 To control for procedural contamination, Milli-Q water was processed in equal
190 conditions as described above for environmental samples. To avoid lab contamination, lab
191 coats were worn during all procedures, slides were washed with acetone, other glassware and
192 filtering devices were thoroughly rinsed with Milli-Q water, pristine plasticware was used
193 (see supplied protocol regarding required precautions during sample handling, such as

194 avoiding low quality pipette tips; fig S4), and Nile red staining solution was freshly filtered
195 through 0.2 μm filters.

196

197 ***Data analysis***

198

199 Automated quantification of fluorescing particles from tow and blank samples was performed
200 in ImageJ using the macro described above. For each sample type, green fluorescence images
201 (109 total) were randomly taken from 5 different filters. Two power-law models were fitted to
202 the particle size distribution with `powerLaw`³⁷ in R. Different x_{min} values were used to
203 estimate the scaling factor: either (1) the smallest particle present in the dataset or (2) an
204 estimate at which the probability distributions of the particle size distribution and the best-fit
205 power-law were most similar above x_{min} .³⁸ The latter discards particles below the estimated
206 x_{min} for which the power-law model is not valid. Testing for other distributions capable of
207 explaining our data was done in accordance with Clauset *et al.*³⁸ Plotting was performed in R
208 using the package `ggplot2`.³⁹

209 A detailed protocol and the code for the macro to semi-automatically quantify
210 fluorescent microplastics in ImageJ are available as supplementary materials.

211 **Results**

212

213 ***Validation of the automated Nile red protocol using commercially available plastics***

214 *Fluorescence assisted counting.* Polymers PE, PP, PS, nylon 6, PC, PET, PVC and PUR
215 fluoresced in green after staining with Nile red (fig. 1) demonstrating the utility of Nile red to
216 detect and quantify small microplastics. Tire rubber did not fluoresce (fig. S1 f). Visual
217 quantification can be performed directly under a microscope, but the implementation of a
218 macro to automate counts allows high throughput counting as well as rapid measurement of
219 the plastic particles. Here, fluorescence based automated detection of microplastics on PCTE
220 membranes was 100 % for 4 polymer types (*i.e.* PE, PP, PS and nylon 6) as all 10 particles of
221 each respective polymer were detected with ImageJ using 29 as the lower threshold for pixel
222 brightness (fig. 1). The other 4 polymers (PUR, PC, PVC and PET) fluoresced weaker and a
223 lower threshold value for pixel brightness (*i.e.* 9) was required to automatically detect all 10
224 particles (fig. 1).

225 As fluorescence intensity varied with polymer type and thickness, the original setting
226 for the pixel brightness threshold (*i.e.* 29) in our macro for ImageJ was optimized to capture
227 all particles with strong fluorescence (*i.e.* PE, PP, PS and nylon 6), and to represent particle
228 size accurately, using brightfield images as size references (figs. 1 & 2). As stated above,
229 100% detection of PUR, PC, PET, and PVC was achieved by lowering the threshold value for
230 pixel brightness. However, the adoption of the lower threshold (1) overestimated the size of
231 more strongly fluorescing particles (*i.e.* PE, PP, PS and nylon 6 in fig. 2), (2) counted strongly
232 fluorescent particles in very close proximity as one unique particle, and (3) so increased the
233 risk of false positives (*i.e.* chitin in fig. 1; discussed below).

234

235 ***Implementation of the fluorescent-staining protocol to environmental samples***

236

237 *Digestion of biogenic material.* Wood lignin fluoresces green and red when stained with Nile
238 red (fig. S2 a). However, particles of this natural polymer, which are below 1 mm in size,

239 were completely eliminated after applying a 7-hour H₂O₂ digestion protocol (fig. S2 b). As
240 with wood lignin, chitin also fluoresces in green and red when stained with Nile red (fig S2
241 c), but was not completely removed during the 7 hour H₂O₂ treatment. Interestingly, after
242 digestion, chitin showed a strong decrease in green fluorescence intensity (but not red
243 fluorescence; fig. S2 d), possibly due to reduced hydrophobicity in response to oxidation. To
244 test whether chitin would interfere with the detection and quantification of synthetic polymers
245 in the green spectrum, we performed our protocol on a mix of chitin and PE. A stark
246 distinction between PE particles and chitin was observed (fig S2 e–g) as the weak
247 fluorescence given by chitin did not interfere when using our highly stringent macro settings
248 (pixel brightness of 29), but chitin is detected to some extent when the settings are brought
249 down (pixel brightness 9). This result highlights two issues that need to be considered when
250 using this protocol: (1) Nile red strongly fluoresces under the GFP settings when staining
251 highly hydrophobic plastics (such as PE, PP, PS) and, hence, green fluorescence should be
252 used to eliminate background and inclusion of natural contaminants; and (2) reducing the
253 sensitivity for the detection of less hydrophobic plastics (e.g. PC, PVC, PUR and PET) can
254 come with a risk of including the detection of particles of natural origin.

255

256 *Detection and quantification of microplastics in environmental samples.* Here we isolated
257 microplastics from environmental samples (*i.e.* beach sediment and sea surface) with
258 saturated NaCl solutions and, hence, expected to extract plastics with densities ≤ 1.2 g/cm³
259 (*e.g.* PE, PP, PS and nylon 6). We applied our Nile red staining protocol to discriminate small
260 microplastic particles from other materials based on fluorescence (fig. 3) as well as to
261 quantify and measure them. The automated ImageJ quantification of microplastics from the
262 sea surface samples using stringent settings resulted in a total of 199 fluorescent particles,
263 ranging between 20 – 338 μ m in size (*i.e.* particle size was obtained from the square root of
264 the area measured for each individual particle; fig. 4). Neither of the power-law models
265 describing the data could be dismissed ($p_{x,\min=20.02} = 0.72$ and $p_{x,\min=101.76} = 0.85$). The particle
266 size distribution followed a power-law more closely for particles >101 μ m, than if all data

267 were used, *i.e.* the smallest particle size = 20 μm (see table S1 for statistical details). The
268 calculated scaling factors were 2.13 for $x_{\text{min}} = 20.02$ and 4.42 for $x_{\text{min}} = 101.76$.

269 Only one fluorescent particle was detected in our negative controls (*i.e.* processed
270 Milli-Q water) demonstrating that laboratory contamination was minimal. It is of uttermost
271 importance to include controls in order to assess the contamination acquired during the
272 processing of samples.

273 For this protocol to be effectively applied to environmental samples we realise it is
274 critical that *only* plastic particles should fluoresce and, hence, be quantified with the semi-
275 automated process. Consequently, we scanned *via* Raman spectroscopy a total of 60
276 fluorescing and non-fluorescing particles and found that all of the fluorescing particles ($n =$
277 37) were of synthetic origin, while all non-fluorescing particles ($n = 23$) gave *non-plastic*
278 Raman signatures (*e.g.* fig. 3). The environmental samples predominantly contained PP-type
279 polymers (83.8%), although PE was also found (16.2%). The Raman spectra of the PP and PE
280 particles contained slight variations in peak structure (fig. S5), which can occur in
281 commercial polymer materials due to the inclusion of additional compounds and pigments or
282 as a consequence of environmental weathering.⁴⁰

283 **Discussion**

284

285 We present a fast, reliable and cost-effective method for detecting, quantifying and
286 determining the size of small PE-, PP-, PS- and nylon 6 type microplastics (20 μm – 1 mm)
287 commonly present in sea surface samples.^{10,11,41} This method uses the lipophilic dye Nile red
288 to fluorescently label plastics and requires fluorescence microscopy to capture images at
289 magnification 10 \times prior to automated, image-based quantification in ImageJ using a macro
290 (both protocol and macro are provided as supplementary information) enabling high
291 throughput image analysis. Specific protocols for collecting and extracting microplastics from
292 the environment were not in the scope of this work.

293 During the preparation of this manuscript, two studies were published^{28,42} that
294 reasserted our findings, demonstrating the effectiveness of Nile red to fluorescently label
295 different types of commercially available synthetic polymers, such as the ones employed here,
296 all of which fluoresce in the green spectrum (black rubber was not used in these previous
297 studies and we show here that it does not fluoresce). Indeed, similarly to us, Shim *et al.*²⁸
298 concluded that green-yellow fluorescence (excitation/emission 450–490/515–565 nm)
299 provided better particle recognition than red or blue fluorescence. Using a different light and
300 filter set-up, Maes *et al.*⁴² reported good fluorescence at longer wavelengths ranging from
301 yellow to orange, depending on the polymer type. Such findings agree with previous reports
302 about the behaviour of Nile red, which favours detection of strongly hydrophobic samples at
303 short excitation/emission wavelengths (450–500/ \leq 580 nm) compared to more neutral lipids,
304 which should ideally be visualised at longer excitation wavelengths (*i.e.* red, 515–560/ \geq 590
305 nm).³⁰ For example, given that PE and PP are more hydrophobic than PET,⁴³ it is expected
306 that the former will fluoresce more intensely at shorter wavelengths (*i.e.* green), while their
307 fluorescence at longer wavelengths remains weak or even absent as we show in figure S1. We
308 are therefore confident that the Nile red protocol we propose here is effective in detecting
309 strongly hydrophobic plastics such as PE, PP, PS and nylon 6 through the use of GFP settings
310 (green fluorescence), while preventing detection of contaminants, that would fluoresce at

311 longer wavelengths. We acknowledge the protocol's limitations for the less hydrophobic
312 polymers PC, PUR, PET and PVC, which constituted about 25% of the European plastic
313 demand in 2015.⁹ These limitations can to some extent be overcome as suggested in the
314 results section by increasing the sensitivity of the method (fig. 1), but this comes at a risk of
315 overestimating the size of strongly fluorescent polymers (fig. 2) as well as incurring the
316 possibility of false positives, such as chitin. It is also worth highlighting that all polymer types
317 that fluoresced weakly in our study when stained with Nile red (PC, PUR, PET, PVC) are
318 denser ($\geq 1.2 \text{ g/cm}^3$) than the polymers that fluoresced more strongly (PE, PP, PS, nylon 6,
319 $< 1.08 \text{ g/cm}^3$). Hence, the latter can be extracted using a saturated NaCl solution as done in
320 this study, while denser polymers would require a higher density salt solution (*e.g.* NaI).

321 The successful application of a Nile red protocol to environmental samples relies on
322 the efficient removal of biogenic particles that could be detected as false positives. As we
323 show here, abundant natural polymers such as chitin and wood lignin fluoresced when stained
324 with Nile red (fig. S2 a, c). Shim *et al.*²⁸ remained cautious on applying Nile red to quantify
325 microplastics in environmental samples due to the risk of co-staining undigested biogenic
326 material. We speculate that the problem they encountered resided in the weak digestion
327 treatment they applied on their beach samples (*i.e.* soaking the filters with 35% H₂O₂), which
328 resulted in biogenic debris such as an amphipod carapace and plant parts still being present.
329 In turn, Shim *et al.*²⁸ reported less such contamination for the neuston net samples, which
330 were digested with the more aggressive Fenton reagent (including heating to 75°C). Hence, a
331 harsh digestion protocol such as the one we used here and which was previously suggested by
332 Claessens *et al.*³¹, is required to prevent co-staining of natural organic polymers and
333 confidently quantify Nile red-stained microplastics in environmental samples. Common
334 plastics such as PE, PP, PS, PET and nylon 6 are resistant to H₂O₂, as demonstrated by Tagg
335 *et al.*³² during a 7-day exposure experiment, where no significant chemical changes were
336 detected *via* FTIR, as opposed to alterations observed elsewhere that were induced by
337 solvents such as acids and bases (*e.g.* HCl or NaOH).^{34,44} In addition to the H₂O₂ digestion, we
338 propose to include a 1 mm mesh-size sieving step prior to the digestion to prevent the

339 inclusion of larger, hard-to-digest natural contaminants, such as amphipods or pieces of
340 wood. If required, enzymatic digestion protocols could be implemented to digest biota-rich
341 environmental samples.^{4,44} Indeed, sample purification may further be optimized by
342 combining digestion procedures with a density separation protocol, such as presented by
343 Maes et al.⁴² Nevertheless, our results show how the 30% H₂O₂ digestion step used here was
344 effective at preventing detection of small natural polymers (below 1 mm in size); wood lignin
345 was completely degraded and chitin was no longer was detectable in ImageJ using green
346 fluorescence images (fig S2). Furthermore, we successfully proved that all of the fluorescing
347 particles from environmental samples assessed with micro-Raman spectroscopy (n = 37) were
348 identified as synthetic plastic materials, whereas no non-fluorescing particles scanned (n =
349 23) showed a synthetic polymer signature.

350 Other semi-automatable methods to detect and quantify small microplastics in
351 environmental samples were recently developed:^{32,45,46}

352 Chemical mapping *via* micro-FTIR was shown useful to detect and identify small
353 microplastics directly on filters when combined with FPA detectors,^{32,45} FPA detectors can
354 record several thousand spectra simultaneously and plastics are then identified based on
355 characteristic bands that are shared by synthetic polymers. However, access to such
356 specialised pieces of equipment is not always possible, and the time required to image a
357 whole filter membrane (10.75 h for a 25 mm diameter filter)⁴⁵ is significantly higher than
358 when using the method in the present study *i.e.* 20 min.

359 A second semi-automatable approach used to detect small microplastics from
360 environmental samples combined Micro-Raman spectroscopy with particle finding
361 software.⁴⁶ The software provides geographical positions of the particles on a slide, and the
362 particles are then scanned individually *via* a motorised stage. However, Frère *et al.*⁴⁶ did not
363 apply this technique directly to the sample filter (such as in this study and others^{32,45}). Instead,
364 particles were visually pre-selected under a dissection microscope and then transferred onto a
365 gold-coated microscope slide. It is therefore not yet clear whether this technique is also
366 applicable to quantify small microplastics without potentially introducing visual bias.

367 While our Nile red staining method does not provide the chemical identity of the
368 detected plastic particles (as achieved *via* FTIR and Raman), we present it as a sensitive, cost-
369 effective and unbiased way of quantifying and measuring small PE, PP, PS and Nylon 6
370 particles in environmental sample preparations to acquire large datasets with high statistical
371 value. Ultimately, a fraction of pinpointed plastic particles should be identified *via* micro-
372 Raman spectroscopy to obtain information on the diversity of polymer types within a sample.
373 Moreover, despite having tested the most common potential natural contaminants, we
374 advocate the use of micro-Raman spectroscopy on subsamples until full reliability of the
375 method presented here has been evaluated.

376 Micro-Raman spectroscopy of plastic particles detected with Nile red showed that PP
377 microparticles were more prevalent (83.8%) in our environmental samples than PE (16.2%).
378 This is notable as PE is the most commonly produced polymer type⁴⁷ and literature highlights
379 PE as the most abundant polymer on sea surfaces.⁴⁸ A recent study, however, found that this
380 is only the case for large microplastics (>1 mm), as the smaller analysed size fraction (0.335 –
381 1 mm) was dominated by PP (42%) rather than PE (26%).⁴⁶ Furthermore, the authors reported
382 a lack of PS in size classes below <2 mm,⁴⁶ which resembles our findings. Curiously, PS was
383 present in the fraction retained by the 1 mm sieve (fig. S3) but not found among particles
384 assessed with Raman. Several non-exclusive hypotheses may explain these findings. For
385 instance, fragmentation behaviours may differ with polymer type and shape. Particles have
386 also been observed to adhere to organic matter, such as marine snow, and sink.^{49,50} It is
387 unclear, however, why small PE particles would more likely be incorporated into marine
388 snow than PP particles, and further research is required to shed light on this interesting
389 phenomenon.

390 Plastics in the environment are known to progressively fragment into smaller
391 particles.² Based on the fragmentation pattern of three dimensional objects, it could be
392 expected that the abundance of microplastic particles increases following a power-law with a
393 factor of 3 as size decreases.⁵ Contrary to this assumption, Cózar *et al.*⁵ reported an intriguing
394 loss in abundance of small microplastics after carrying out a global survey of sea surface

395 marine plastic debris. The expected correlation between size and fragment abundance was
396 observed down to a particle size of 2 mm but, surprisingly, the abundance of microplastics
397 sharply decreased for particles below 1 mm in size. This supported speculation regarding the
398 substantial ‘missing’ fraction of marine plastic debris initiated in 2004,¹⁴ and recently
399 reviewed by Eriksen *et al.*⁵¹ We believe that the extremely low incidence of small
400 microplastics reported by Cózar *et al.*⁵ may partly be ascribed to the methods employed in
401 identifying and selecting particles, which were based on visual sorting under a dissecting
402 microscope. In fact, in a study whose findings mirrored our own, Enders *et al.*⁵² showed that
403 small microplastics were indeed present in surface waters with increasing abundance as size
404 decreased, and obtained a scaling factor of 1.96 for the size range of 10 – 110 μm , close to
405 one obtained in this study (*i.e.* scaling factor of 2.13). Further research is nevertheless
406 required, as very little is known about the fragmentation pattern and particle behaviour of
407 different polymer types in the marine environment.⁵³

408 Here we suggest the use of a highly sensitive Nile red fluorescent staining method for
409 identifying the smaller size range of lower density microplastics (<1 mm) commonly present
410 in sea surface samples (*i.e.* PE, PP, PS and nylon 6). We acknowledge its limitations, but do
411 not exclude its application, for less hydrophobic polymer types, a separation that coincides
412 with higher polymer densities (>1.2 g/cm^3 ; fig. 1). Using this time- and cost-effective
413 protocol to quantify and measure small microplastics allowed us to confirm that small
414 microplastics are increasingly abundant with decreasing particle size in sea surface samples
415 (fig. 4). This method therefore addresses the quantification uncertainties and provides an
416 effective tool for rapid quantification of small microplastics by substituting the visual
417 selection and quantification process with an automated process.

418

419 **Supporting Information**

420 Five figures (green and red fluorescence, Nile red stained natural polymers, microplastics >1
421 mm, contamination control, example Raman spectra of microplastics from environmental

422 samples), one table with statistical details, a sample preparation protocol and the code for the

423 ImageJ script used to quantify fluorescent microplastic particles; all as noted in the text

424

425

426 Acknowledgements

427 This work was supported by the NERC Independent Research Fellowship NE/K009044/1.
428 The microscope facility was provided by WISB, which is a BBSRC/EPSRC Synthetic
429 Biology Research Centre (grant ref.: BB/M017982/1) funded under the UK Research
430 Councils' Synthetic Biology for Growth programme. Gabriel Erni Cassola was supported by a
431 NERC CENTA PhD studentship. We thank skipper Richard Ticehurst (Plymouth University)
432 for his help and expertise during field work. Special thanks go to Vinko Zadjelovic and
433 Robyn Wright for providing input throughout the study. The authors declare no conflict of
434 interest.

435

436 Author contributions

437 G.E.C., J.C.-O. and M.I.G. conceived the study. G.E.C. designed and conducted the
438 experimental work. R.C.T. provided expertise and advice on fieldwork, microplastic
439 identification and gave access to the facilities. G.E.C. and J.C.-O. analysed the data and wrote
440 the paper. M.I.G. and R.C.T. provided their expertise and reviewed the manuscript.

441 **References**

- 442 (1) Jambeck, J. R.; Geyer, R.; Wilcox, C.; Siegler, T. R.; Perryman, M.; Andrady, A.;
443 Narayan, R.; Law, K. L. Plastic waste inputs from land into ocean. *Science (80-.)*.
444 **2015**, *347* (6223), 768–771.
- 445 (2) Barnes, D. K. A.; Galgani, F.; Thompson, R. C.; Barlaz, M. Accumulation and
446 fragmentation of plastic debris in global environments. *Phil. Trans. R. Soc. B* **2009**,
447 *364*, 1985–1998.
- 448 (3) Wright, S. L.; Thompson, R. C.; Galloway, T. S. The physical impacts of
449 microplastics on marine organisms: A review. *Environ. Pollut.* **2013**, *178*, 483–492.
- 450 (4) Mani, T.; Hauk, A.; Walter, U.; Burkhardt-Holm, P. Microplastics profile along the
451 Rhine River. *Sci. Rep.* **2015**, *5*, 17988.
- 452 (5) Cózar, A.; Echevarría, F.; González-Gordillo, J. I.; Irigoien, X.; Ubeda, B.;
453 Hernández-León, S.; Palma, A. T.; Navarro, S.; García-de-Lomas, J.; Ruiz, A.; et al.
454 Plastic debris in the open ocean. *PNAS* **2014**, *111*, 10239–10244.
- 455 (6) Woodall, L. C.; Sanchez-Vidal, A.; Canals, M.; Paterson, G. L. J.; Coppock, R.;
456 Sleight, V.; Calafat, A.; Rogers, A. D.; Narayanaswamy, B. E.; Thompson, R. C. The
457 deep sea is a major sink for microplastic debris. *R. Soc. Open Sci.* **2014**, *1* (4), 140317.
- 458 (7) Claessens, M.; Meester, S. De; Landuyt, L. Van; Clerck, K. De; Janssen, C. R.
459 Occurrence and distribution of microplastics in marine sediments along the Belgian
460 coast. *Mar. Pollut. Bull.* **2011**, *62* (10), 2199–2204.
- 461 (8) Pedrotti, M. L.; Petit, S.; Elineau, A.; Bruzard, S.; Crebassa, J.-C.; Dumontet, B.;
462 Martí, E.; Gorsky, G.; Cózar, A. Changes in the Floating Plastic Pollution of the
463 Mediterranean Sea in Relation to the Distance to Land. *PLoS One* **2016**, *11* (8),
464 e0161581.
- 465 (9) PlasticsEurope. Plastic - the facts 2016. *Brussels* **2016**.
- 466 (10) Suaria, G.; Avio, C. G.; Mineo, A.; Lattin, G. L.; Magaldi, M. G.; Belmonte, G.;
467 Moore, C. J.; Regoli, F.; Aliani, S. The Mediterranean Plastic Soup: synthetic
468 polymers in Mediterranean surface waters. *Sci. Rep.* **2016**, *6*, 37551.
- 469 (11) Gajšt, T.; Bizjak, T.; Palatinus, A.; Liubartseva, S.; Kržan, A. Sea surface
470 microplastics in Slovenian part of the Northern Adriatic. *Mar. Pollut. Bull.* **2016**, *113*,
471 392–399.
- 472 (12) Eriksen, M.; Lebreton, L. C. M.; Carson, H. S.; Thiel, M.; Moore, C. J.; Borerro, J. C.;
473 Galgani, F.; Ryan, P. G.; Reisser, J. Plastic Pollution in the World's Oceans: More
474 than 5 Trillion Plastic Pieces Weighing over 250,000 Tons Afloat at Sea. *PLoS One*
475 **2014**, *9* (12), e111913.
- 476 (13) Cózar, A.; Sanz-Martín, M.; Martí, E.; González-Gordillo, J. I.; Ubeda, B.; Gálvez, J.
477 Á.; Irigoien, X.; Duarte, C. M. Plastic Accumulation in the Mediterranean Sea. *PLoS*
478 *One* **2015**, *10* (4), e0121762.
- 479 (14) Thompson, R. C.; Olsen, Y.; Mitchell, R. P.; Davis, A.; Rowland, S. J.; John, A. W.
480 G.; McGonigle, D.; Russell, A. E. Lost at sea: where is all the plastic? *Science (80-.)*.
481 **2004**, *304* (5672), 838.
- 482 (15) Moore, C. J. Synthetic polymers in the marine environment: A rapidly increasing,
483 long-term threat. *Environ. Res.* **2008**, *108*, 131–139.
- 484 (16) Browne, M. A.; Crump, P.; Niven, S. J.; Teuten, E.; Tonkin, A.; Galloway, T.;
485 Thompson, R. Accumulation of microplastic on shorelines worldwide: Sources and
486 sinks. *Environ. Sci. Technol.* **2011**, *45* (21), 9175–9179.
- 487 (17) Corcoran, P. L.; Biesinger, M. C.; Griffi, M. Plastics and beaches: A degrading
488 relationship. *Mar. Pollut. Bull.* **2009**, *58* (1), 80–84.
- 489 (18) Andrady, A. L. Microplastics in the marine environment. *Mar. Pollut. Bull.* **2011**, *62*
490 (8), 1596–1605.
- 491 (19) Morét-Ferguson, S.; Lavender, K.; Proskurowski, G.; Murphy, E. K.; Peacock, E. E.;
492 Reddy, C. M. The size, mass, and composition of plastic debris in the western North
493 Atlantic Ocean. *Mar. Pollut. Bull.* **2010**, *60*, 1873–1878.
- 494 (20) Setälä, O.; Fleming-Lehtinen, V.; Lehtiniemi, M. Ingestion and transfer of
495 microplastics in the planktonic food web. *Environ. Pollut.* **2014**, *185*, 77–83.

- 496 (21) Watts, A. J. R.; Lewis, C.; Goodhead, R. M.; Beckett, S. J.; Moger, J.; Tyler, C. R.;
497 Galloway, T. S. Uptake and Retention of Microplastics by the Shore Crab *Carcinus*
498 *maenas*. *Environ. Sci. Technol.* **2014**, *48* (15), 8823–8830.
- 499 (22) Teuten, E. L.; Saquing, J. M.; Knappe, D. R. U.; Barlaz, M. A.; Jonsson, S.; Björn, A.;
500 Rowland, S. J.; Thompson, R. C.; Galloway, T. S.; Yamashita, R.; et al. Transport and
501 release of chemicals from plastics to the environment and to wildlife. *Philos. Trans. R.*
502 *Soc. B* **2009**, *364*, 2027–2045.
- 503 (23) Rochman, C. M.; Kross, S. M.; Armstrong, J. B.; Bogan, M. T.; Darling, E. S.; Green,
504 S. J.; Smyth, A. R.; Veríssimo, D. Scientific Evidence Supports a Ban on Microbeads.
505 *Environ. Sci. Technol.* **2015**, *49* (18), 10759–10761.
- 506 (24) Hanke, G.; Galgani, F.; Werner, S.; Oosterbaan, L.; Nilsson, P.; Fleet, D.; Kinsey, S.;
507 Thompson, R.; Palatinus, A.; Franeker, J. A. Van; et al. *MSFD GES technical*
508 *subgroup on marine litter. Guidance on monitoring of marine litter in European Seas.*;
509 Luxembourg, 2013.
- 510 (25) Hidalgo-Ruz, V.; Gutow, L.; Thompson, R. C.; Thiel, M. Microplastics in the Marine
511 Environment: A Review of the Methods Used for Identification and Quantification.
512 *Environ. Sci. Technol.* **2012**, *46*, 3060–3075.
- 513 (26) Lavers, J. L.; Oppel, S.; Bond, A. L. Factors influencing the detection of beach plastic
514 debris. *Mar. Environ. Res.* **2016**, *119*, 245–251.
- 515 (27) Andrady, A. L. Using flow cytometry to detect micro- and nano-scale polymer
516 particles. In *Proceedings of the Second Research Workshop on Microplastic Debris.*;
517 Arthur, C., Baker, J., Eds.; NOAA Technical Memorandum NOS-OR&R-39., 2010.
- 518 (28) Shim, W. J.; Song, Y. K.; Hong, S. H.; Jang, M. Identification and quantification of
519 microplastics using Nile Red staining. *Mar. Pollut. Bull.* **2016**, *113*, 469–476.
- 520 (29) Cole, M. A novel method for preparing microplastic fibers. *Sci. Rep.* **2016**, *6*, 34519.
- 521 (30) Rumin, J.; Bonnefond, H.; Saint-Jean, B.; Rouxel, C.; Sciandra, A.; Bernard, O.;
522 Cadoret, J.-P.; Bougaran, G. The use of fluorescent Nile red and BODIPY for lipid
523 measurement in microalgae. *Biotechnol. Biofuels* **2015**, *8*, 42.
- 524 (31) Claessens, M.; Van Cauwenberghe, L.; Vandegehuchte, M. B.; Janssen, C. R. New
525 techniques for the detection of microplastics in sediments and field collected
526 organisms. *Mar. Pollut. Bull.* **2013**, *70* (1–2), 227–233.
- 527 (32) Tagg, A. S.; Sapp, M.; Harrison, J. P.; Ojeda, J. J. Identification and Quantification of
528 Microplastics in Wastewater Using Focal Plane Array-Based Reflectance Micro-FT-
529 IR Imaging. *Anal. Chem.* **2015**, *87* (12), 6032–6040.
- 530 (33) Zimmermann, W.; Paterson, A.; Broda, P. Preparation of Milled Straw Lignin from
531 Barley. *Methods Enzymol.* **1988**, *161*, 191–199.
- 532 (34) Nuelle, M.-T.; Dekiff, J. H.; Remy, D.; Fries, E. A new analytical approach for
533 monitoring microplastics in marine sediments. *Environ. Pollut.* **2014**, *184*, 161–169.
- 534 (35) Team, R. C. R Core Team 2015 R: A language and environment for statistical
535 computing. R foundation for statistical computing. **2015**, 2014.
- 536 (36) Liland, K. H.; Mevik, B.-H.; Canteri, R. baseline: Baseline Correction of Spectra.
537 2015.
- 538 (37) Gillespie, C. S. Fitting heavy tailed distributions: the powerLaw package. *J. Stat.*
539 *Softw.* **2015**, *64* (2), 1–16.
- 540 (38) Clauset, A.; Shalizi, C. R.; Newman, M. E. J. Power-Law distributions in empirical
541 data. *Soc. Ind. Appl. Math.* **2009**, *51* (4), 661–703.
- 542 (39) Wickham, H. *ggplot2*; Gentleman, R., Hornik, K., Parmigiani, G., Eds.; Springer,
543 2009.
- 544 (40) Lenz, R.; Enders, K.; Stedmon, C. A.; Mackenzie, D. M. A.; Gissel, T. A critical
545 assessment of visual identification of marine microplastic using Raman spectroscopy
546 for analysis improvement. *Mar. Pollut. Bull.* **2015**, *100* (1), 82–91.
- 547 (41) Ballent, A.; Corcoran, P. L.; Madden, O.; Helm, P. A.; Longstaffe, F. J. Sources and
548 sinks of microplastics in Canadian Lake Ontario nearshore, tributary and beach
549 sediments. *Mar. Pollut. Bull.* **2016**, *110* (1), 383–395.
- 550 (42) Maes, T.; Jessop, R.; Wellner, N.; Haupt, K.; Mayes, A. G. A rapid-screening

- 551 approach to detect and quantify microplastics based on fluorescent tagging with Nile
552 Red. *Sci. Rep.* **2017**, *7*, 44501.
- 553 (43) Dodbiba, G.; Haruki, N.; Shibayama, A.; Miyazaki, T.; Fujita, T. Combination of
554 sink–float separation and flotation technique for purification of shredded PET-bottle
555 from PE or PP flakes. *Int. J. Miner. Process.* **2002**, *65*, 11–29.
- 556 (44) Cole, M.; Webb, H.; Lindeque, P. K.; Fileman, E. S.; Halsband, C.; Galloway, T. S.
557 Isolation of microplastics in biota-rich seawater samples and marine organisms. *Sci.*
558 *Rep.* **2014**, *4*, 4528.
- 559 (45) Löder, M. G. J.; Kuczera, M.; Mintenig, S.; Lorenz, C.; Gerdt, G. Focal plane array
560 detector-based micro-Fourier-transform infrared imaging for the analysis of
561 microplastics in environmental samples. *Environ. Chem.* **2015**, *12* (5), 563–581.
- 562 (46) Frère, L.; Paul-Pont, I.; Moreau, J.; Soudant, P.; Lambert, C.; Huvet, A.; Rinnert, E. A
563 semi-automated Raman micro-spectroscopy method for morphological and chemical
564 characterizations of microplastic litter. *Mar. Pollut. Bull.* **2016**, *113* (1–2), 461–468.
- 565 (47) PlasticsEurope. *Plastics - the facts 2015*; Brussels, 2015.
- 566 (48) Phuong, N. N.; Zalouk-Vergnoux, A.; Poirier, L.; Kamari, A.; Châtel, A.; Mouneyrac,
567 C.; Lagarde, F. Is there any consistency between the microplastics found in the field
568 and those used in laboratory experiments? *Environ. Pollut.* **2016**, *211*, 111–123.
- 569 (49) Long, M.; Moriceau, B.; Gallinari, M.; Lambert, C.; Huvet, A.; Raffray, J.; Soudant,
570 P. Interactions between microplastics and phytoplankton aggregates: Impact on their
571 respective fates. *Mar. Chem.* **2015**, *175*, 39–46.
- 572 (50) Zhao, S.; Danley, M.; Ward, J. E.; Mincer, T. J. An approach for extraction,
573 characterization and quantitation of microplastic in natural marine snow using Raman
574 microscopy. *Anal. Methods* **2017**, *9*, 1470–1478.
- 575 (51) Eriksen, M.; Thiel, M.; Lebreton, L. Nature of Plastic Marine Pollution in the
576 Subtropical Gyres. In *The Handbook of Environmental Chemistry*; Takada, H.,
577 Karapanagioti, H. K., Eds.; Springer Berlin Heidelberg, 2016; pp 1–28.
- 578 (52) Enders, K.; Lenz, R.; Stedmon, C. A.; Nielsen, T. G. Abundance, size and polymer
579 composition of marine microplastics $\geq 10 \mu\text{m}$ in the Atlantic Ocean and their
580 modelled vertical distribution. *Mar. Pollut. Bull.* **2015**, *100*, 70–81.
- 581 (53) Filella, M. Questions of size and numbers in environmental research on microplastics:
582 Methodological and conceptual aspects. *Environ. Chem.* **2015**, *12* (5), 527–538.
583

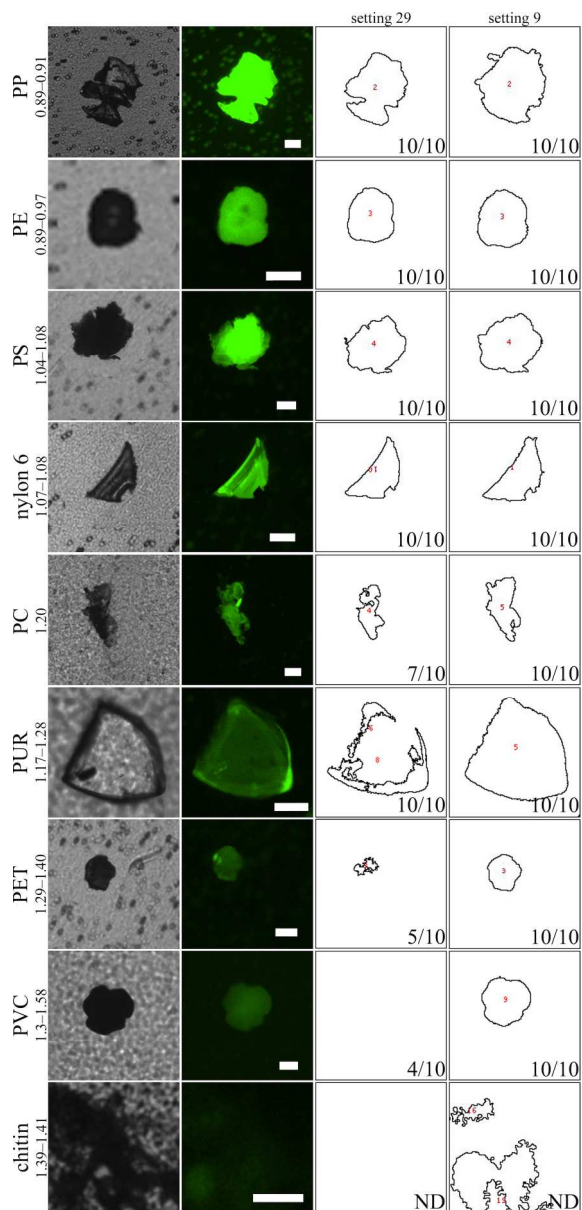


Figure 1. Microscope and ImageJ images of microparticles of different polymer types on PCTE filter membranes stained with Nile red. For each polymer, images show from left to right: a particle in brightfield, the same particle in green fluorescence (excitation/emission 460/525 nm), ImageJ rendition with stringent settings (setting 29) and ImageJ rendition with more sensitive settings (setting 9). Ratios in ImageJ renditions indicate the number of particles ($n = 10$) detected with the respective setting and polymer; ND: not determined. Polymers are in descending order in accordance with increasing specific density (g/cm^3), indicated below polymer name; PP: polypropylene, PE: polyethylene, PS: polystyrene, PC: polycarbonate, PUR: polyurethane, PET: poly(ethylene terephthalate), PVC: poly(vinyl carbonate). Scale = 50 μm .

136x289mm (300 x 300 DPI)

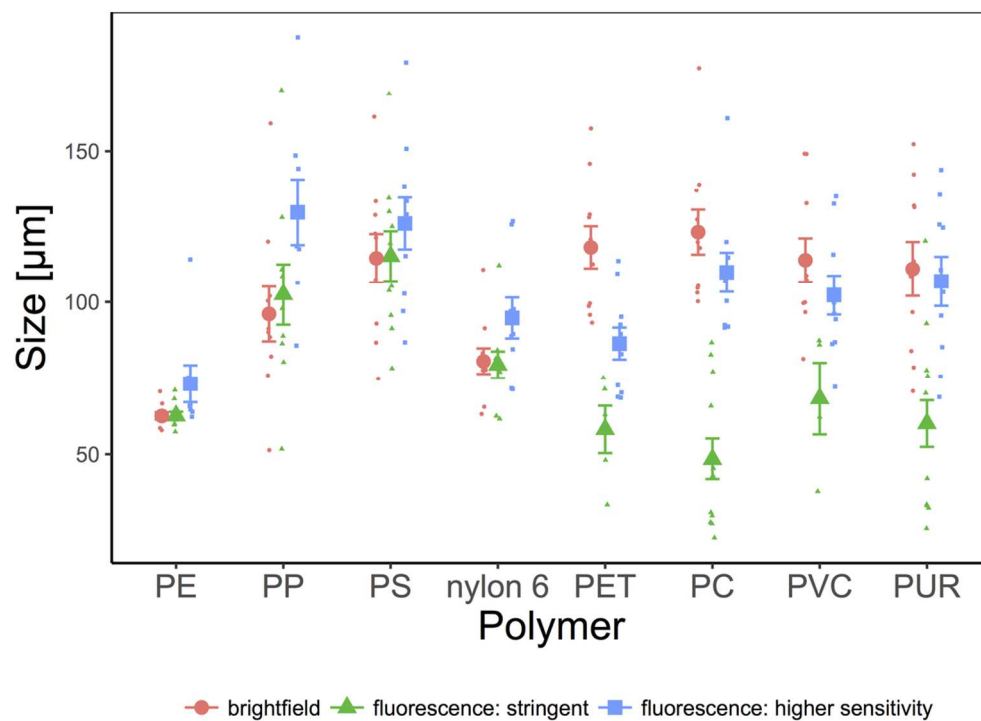


Figure 2. Mean size (\pm SE) comparison of microplastic particle ($n = 10$ per polymer type) size measured in ImageJ using either brightfield images or green fluorescence images with our script. Note: stringent represents sizes measured with 29 as the lower threshold for pixel brightness and higher sensitivity corresponds to measurements generated with 9 as the lower threshold for pixel brightness. Size corresponds to the square root of particle area.

109x83mm (300 x 300 DPI)

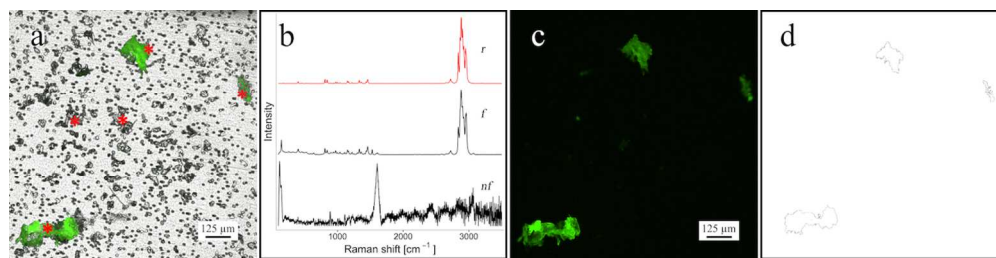


Figure 3. Microscope images of processed sand samples demonstrating selective Nile red fluorescent staining of synthetic polymers with Raman spectra of scanned particles. (a) Composite image of excitation/emission 460/525 nm and brightfield. Asterisks indicate particles assessed via Raman-spectroscopy. (b) Normalised Raman spectra obtained from particles highlighted in image b. r: PP (Sigma-Aldrich) spectrum; f: typical spectrum of fluorescent particle in image b; nf: typical spectrum of non-fluorescing particle in image b. (c) Field shown in panel (a) using green fluorescence only. (d) ImageJ drawing depicting particles $>400 \mu\text{m}^2$ that were quantified via our macro.

117x29mm (300 x 300 DPI)

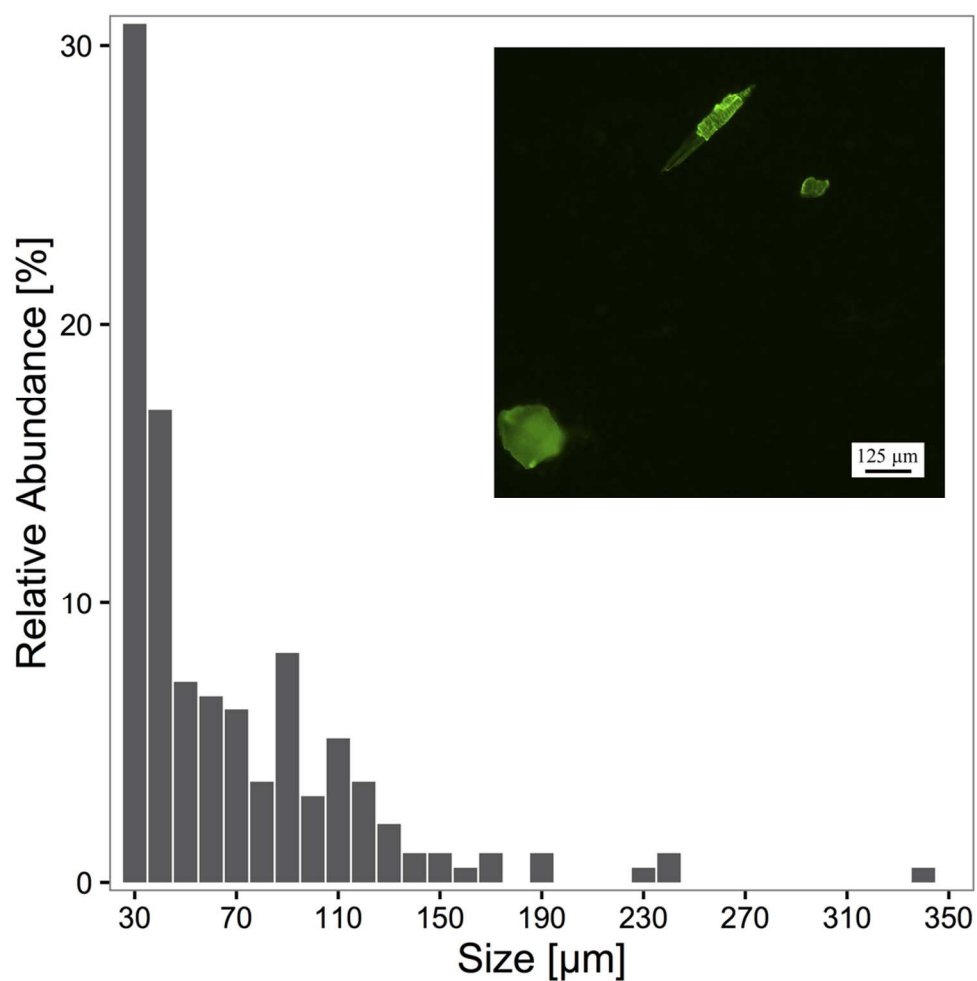
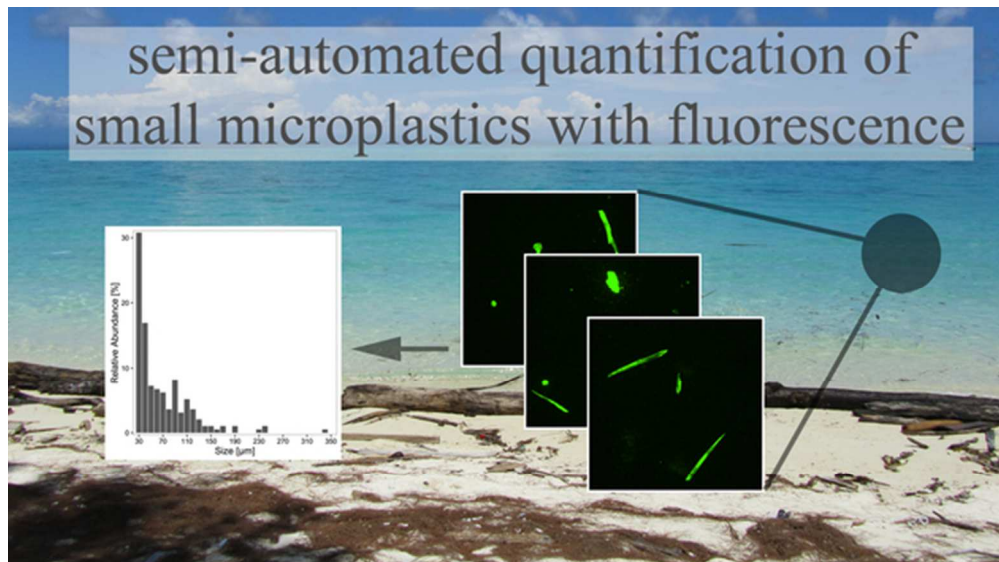


Figure 4. Relative abundance of microplastic particle sizes ($n_p = 199$) from all sea surface samples analysed via automated counting of fluorescent particles using 109 different microscope fields (one image shown as example). Size corresponds to the square root of the particle's area.

99x99mm (300 x 300 DPI)



abstract art

26x15mm (600 x 600 DPI)